Interconnected Interpenetrating Polymer Networks of Polyurethane and Polystyrene. 2. Structure–Property Relationships†

S. B. Pandit, S. S. Kulkarni, and V. M. Nadkarni*

Polymer Science and Engineering Group, Chemical Engineering Division, National Chemical Laboratory, Pune 411 008, India

Received September 3, 1993; Revised Manuscript Received December 29, 1993•

ABSTRACT: This paper discusses the properties of interconnected interpenetrating polymer networks (IPNs) based on polyurethane (PU) and polystyrene (PS), formed by varying the PU/PS ratio. The interconnected IPNs were prepared by first forming a PU network based on an unsaturated polyester polyol with toluene diisocyanate in the presence of a triol, followed by interconnecting the PU chain segments by reaction of styrene with sites of unsaturation. Five such IPNs have been prepared at PU/PS ratios of 100/0, 90/10, 80/20, 70/30, and 50/50. The properties of these IPNs have been rationalized on the basis of the structure of these IPNs reported in an earlier communication. The mechanical properties, namely, tensile strength at break and elongation at break, have been shown to correlate well with the cross-link factor (CLF) of the IPNs. CLF is a measure of the number of cross-link points per gram of the resin. The tensile recovery behavior has been explained on the basis of the morphology of the IPNs. The dynamic mechanical analysis of the interconnected IPNs having a PS content up to 30% have shown only one glass transition temperature (T_g) corresponding to the PU phase. The T_g of the PS phase was not observed in the temperature range employed. In the case of IPN containing 50/50 PU/PS, two T_g's were observed corresponding to PU and PS phases due to the coiled configuration of the PS bridges. The dependence of the Molecular weight between cross-links (M_c) of the IPNs on the PS concentration showed a trend similar to that of the CLF. The permeability studies showed that the flux of N_2 and CO_2 gases through the IPNs is governed by the cross-link density and the morphology of the IPNs. The thermal degradation behavior of the IPNs was rationalized on the basis of the structure.

Introduction

Interpenetrating polymer networks (IPNs) have been extensively investigated over the past two decades due to their ability to produce versatile materials with the required combination of properties.[1] IPNs represent structurally complex polymer systems, since their structure can be changed not only through the use of a variety of chemical building blocks but also by following various sequences of preparation to manipulate the relative rates of network formation. The structure–property relationships of IPNs have been therefore studied in order to find out the effect of various variables on the properties without elucidating the complex structure of the IPNs. Thus, mechanical behavior,[2] dynamic mechanical behavior,[3] degradation behavior,[4] and barrier properties[5] of IPNs have been thoroughly investigated by changing the composition of IPNs, levels of interconnection between the networks, degree of cross-linking, method of preparation, etc. It has been shown that intranetwork bridges formed in the interconnected IPNs can greatly affect the IPN structure and properties. Sperling et al.[6] have shown that relatively low levels of grafting can cause significant changes in morphology and behavior of the final product. A similar observation was made by Frisch et al.[7] in the case of epoxy/acrylic IPNs with intentional grafts.

In our earlier communication[8] we have proposed the structure of interonnected IPNs based on polyurethane (PU) and polystyrene (PS). The present paper discusses the variation of properties of these IPNs with structural parameters such as extent of cross-linking, network cage size, etc. and their rationalization on the basis of the proposed structure.

* To whom all correspondence should be addressed. Current address: Performance Polymers Pvt. Ltd., 10 Narendra Society, Senapati Bapat Rd., Pune 411 016, India.

† NCL Communication No. 5853.

• Abstract published in *Advance ACS Abstracts*, February 15, 1994.

Experimental Section

Synthesis. The materials and procedure used for the synthesis of the IPNs are reported in an earlier communication[8] and hence will be discussed briefly.

IPN Synthesis. The IPNs were synthesized by varying the PU/PS ratios. The PU component was formed by reacting the mixture of 4 hydroxyl equiv of unsaturated polyester polyol PUP-2 and 1 hydroxyl equiv of trimethylol propane (TMP) with 5 isocyanate equiv of tolylene diisocyanate and the PS component consisted of styrene containing 2% benzoyl peroxide. The detailed synthetic procedure of unsaturated polyester polyol PUP-2 has been discussed in an earlier communication.[8]

Unsaturated polyester polyol PUP-2 (4 hydroxyl equiv) and 1 hydroxyl equiv of TMP were mixed in a degassing chamber. The mixture was heated to 70 °C to dissolve the TMP in PUP-2 and degassed at 80 °C for 1 h with mechanical stirring at a reduced pressure of 1–2 Torr. The mixture was then cooled to room temperature and 5 isocyanate equiv of TDI was added. The reaction mixture was mixed thoroughly and degassed further for 5 min.

In a separate beaker, the desired amount of styrene monomer containing 2% BPO was weighed and the required quantity of the degassed PU was added to this mixture under constant stirring to obtain a homogeneous mixture which was then cast into an open aluminum mold of size 250 mm × 250 mm × 2 mm.

The IPNs were cured at room temperature for 24 h to complete the PU network formation, followed by a postcure at 90 ± 2 °C for 20 h and at 120 ± 2 °C for 6 h to complete the polymerization of styrene. Using this procedure, five IPNs were prepared by varying the PU/PS (w/w) ratios of 100/0, 90/10, 80/20, 70/30, and 50/50 and were coded as PU-2, IS1A, IS1B, IS1C, and IS1D, respectively. The isocyanate index of all the PU compositions was kept constant at 100.

Characterization and Testing. Wide Angle X-ray Diffraction (WAXD). The solid state morphology of the IPNs was studied using wide angle X-ray diffraction. Wide angle X-ray diffraction studies were carried out using the Philips PW 1730 X-ray generator unit. The X-rays of 1.54-Å wavelength were generated using a Cu Kα source. The angle of diffraction (2θ) was varied from 4 to 35°.

Mechanical Properties. The hardness of the IPN samples was tested using a Shore A hardness tester, at a minimum sample thickness of 6 mm. The tensile test specimens were cut from a

0024-9297/94/2227-4595$04.50/0

2-3-mm-thick IPN sheet using a die cutter of ASTM D-412 type C size. All specimens were about 2-3 mm thick. At least four specimens of each IPN sample were tested. The measurements were taken on an Instron tensile tester, Model 1122, at two deformation rates of 20 and 50 mm/min (i.e. 50 and 125% elongation/min since the gauge length was 40 mm). All the measurements were done at 25 °C.

Dynamic Mechanical Analysis (DMA). The viscoelastic behavior of the IPNs was studied using the dynamic mechanical analyzer Rheometrics RDS 7800. The specimens were cut into 1.2 cm × 6.0 cm × 0.2–0.3 cm size. The sample was clamped vertically in the two arms of the instrument. The torsional strain amplitude was oscillated up to 0.5% at a frequency of 100 rad/s. The data were collected in the temperature range −70 to +130 °C at a heating rate of 10 °C/min in the cure mode. Liquid nitrogen (temperature −196 °C) was used to achieve subambient temperatures.

Permeability. For the permeability studies IPN films were cast from a 15% (w/w) solution of monomers (both PU and PS) in acetone. This solution was cast on a mercury filled Petri dish and cured at room temperature for 24 h followed by a postcure at 90 °C for 24 h. The average thickness of the films was 150 μm. The film thickness was measured with a vernier gauge. The polymer films were cut into disks of 2.5-cm diameter and were placed in the permeability apparatus.[9] The permeability was measured after steady state conditions were reached. The permeabilities of all the samples were measured at 35 °C and at a pressure ~300 psi, for N_2 and CO_2 gases. The permeability of CO_2 was also measured as a function of pressure (200–400 psi) for the samples PU-2 and IS1C. Both N_2 and CO_2 were procured from M/S Indian Oxygen Ltd. and were 99% pure. Both gases were used without further purification. The activation energy of N_2 passage through IPN IS1C was calculated from the permeabilities at various temperatures from 7 to 80 °C.

Thermogravimetric Analysis. The thermal and oxidative degradation behavior of the IPNs was studied using a Netzch STA-409 Thermal Analyzer. The IPNs were cut in small pieces using a razor blade. About 20 mg of sample was taken and heated at a constant rate of 10 °C/min in air (oxidative environment).

Results and Discussion

In our earlier communication,[8] a detailed study aimed at elucidating the structure of the interconnected IPNs, was reported. It was shown that these IPNs can be classified into three groups on the basis of their structure. The PU network of PU-2 is formed by amorphous chains of polyurethanes, as shown in Figure 1. The networks of IPNs IS1A, IS1B, and IS1C are formed by accommodating the stretched PS bridges into the cages of the PU network, and as a result, the chains of the PU are also stretched; this is schematically depicted in Figure 1. It was observed that the stretching of PU chains leads to strain-induced crystallization of the polyether chain segments. In the case of IPN IS1D containing longer PS bridges, the PS intranetwork bridges are accommodated in the PU cages in a coiled configuration and a collapsed cage network is formed (Figure 1). However, it has been shown in an earlier communication that these coiled PS bridges, present in IS1D, can be transformed into a stable stretched configuration by stretching the IPN network up to 50% elongation and holding it stretched for 1 h.

The network structure is governed by the type and extent of cross-linking. A cross-link factor (CLF) was defined to represent the cage structure in a quantitative manner.[8] CLF is a number representing the cross-linking density of the IPN if all the styrene was used in forming intranetwork bridges. While the CLF was being defined, it was assumed that the reaction between -OH groups and -NCO is complete; no linkages except urethane formation takes place at an isocyanate index of 100; and the reactive double bonds present in the PU network do not undergo oxidative cross-linking during the α-stage cure. Using these assumptions the CLF was defined as follows:

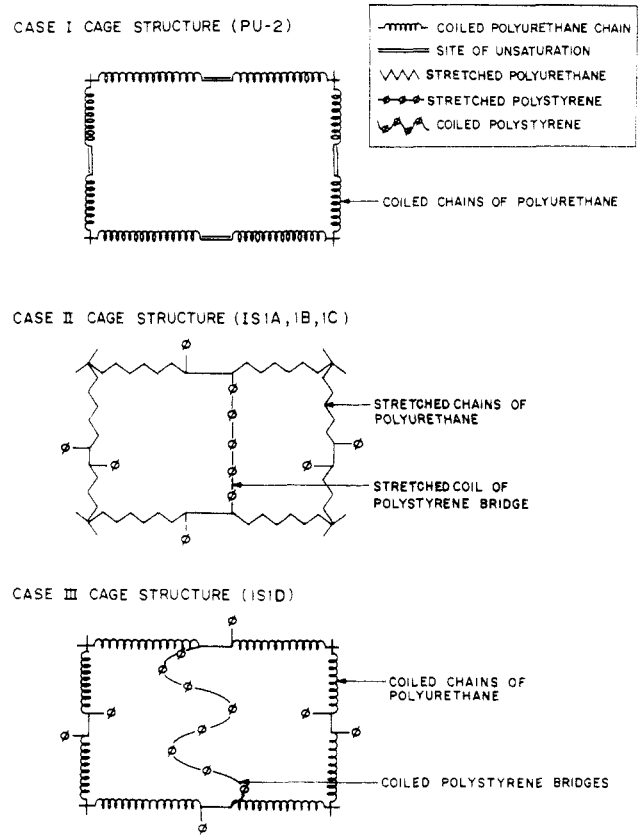

Figure 1. Hypothesized structures of the IPNs.

$$\mathrm{CLF} = \left[C_u\left(\frac{\mathrm{II}}{100}\right)^f + C_s + 0.5D_b\left(\frac{\mathrm{II}}{100}\right)^2 + 2E_i\right] \times 10^4 \quad (1)$$

where C_u is the moles of PU cross-linker per gram of formulation (for example TMP), II is the isocyanate index, f is the functionality of the PU cross-linker ($f = 3$ for TMP), C_s is the moles of styrene cross-linker per gram of formulation, D_b is the moles of double bond present in PU per gram of formulation, and E_i is the moles of excess isocyanate groups present per gram of formulation (applicable at II > 100). At isocyanate indices of less than 100, some of the cages are not completely formed due to formation of an infinite network containing a large number of dangling chains with -OH end groups. The factors $(\mathrm{II}/100)^f$ and $(\mathrm{II}/100)^2$ signify the probability that the cross-linker of functionality f and the sites of unsaturation will act as an effective cross-link. Thus, these probabilities are valid only for the IPNs containing the PU networks formed with an isocyanate index of less than 100. If the isocyanate index of the PU network exceeds 100, then this factor should be eliminated from the equation. At an isocyanate index greater than 100, excess isocyanate groups are present which form allophanate linkages. The term E_i signifies the probability of formation of cross-link points due to allophanate linkages. The amount of double bonds was normalized by multiplying with 0.5, as only 50% of the double bonds is available for reaction with styrene.[8] From a phenomenological viewpoint, the network cage size decreases with the increasing CLF value.

Using the same assumptions, the average number of styrene monomer units constituting the PS bridges was calculated in terms of moles of styrene present per mole of site of unsaturation in the PU network chains. This bridge length is expressed in terms of the number of styrene units (SU). The CLF and the intranetwork bridge lengths of PS for all the IPNs are tabulated in Table 1.

Table 1. Cross-Link Factor (CLF), Bridge Lengths, and d_{eff} of IPNs

code	PU/PS (w/w)	cross-link factor	bridge length (SU)	d_{eff} (Å)
PU-2	100/00	2.07		4.04
IS1A	90/10	8.33	1.49	4.15
IS1B	80/20	7.40	3.35	4.15
IS1C	70/30	6.48	5.63	4.19
IS1D	50/50	4.63	13.4	3.96

The wide angle X-ray diffraction (WAXD) study was carried out to investigate the solid state structure of the IPNs in terms of the cage size. The effective distance between the chains, d_{eff}, for these IPNs was calculated from the location of the amorphous peak observed using WAXD. d_{eff} is a measure of intersegmental distance between the polymer chains present in the solid state. The values of d_{eff} are listed in Table 1. It was observed that the d_{eff} increases with increasing PS content due to the stretching of the PU network by polystyrene intranetwork bridges. A maxima in d_{eff} was observed for the IPN, IS1C, having an intranetwork bridge length of 5.7 SU; this was accompanied by crystalline peaks, indicating that the polyether chains present in the PU network are crystallized. On further increase of the bridge length to 13.4 SU, in the IPN, IS1D, the d_{eff} decreased significantly to a value lower than the d_{eff} of the base PU network, PU-2. This show that the PS bridges which are present as stretched chains lead to stretching of the flexible PU cages, thus increasing the d_{eff}. In the case of IS1D, a longer intranetwork bridge length led to the formation of a collapsed cage morphology with coiled PS chains. This resulted in a large decrease in d_{eff}.

The hardness, tensile properties, dynamic mechanical behavior, thermal stability, and permeability characteristics of the IPNs are highly sensitive to its chemical composition, physical structure, and domain morphology. The dependence of these properties on the structure parameters, such as CLF, bridge length of the PS intranetwork bridges, d_{eff}, and crystallinity, are reported in this paper.

Mechanical Properties. The hardness of the base PU network was found to increase sharply with a 10% addition of styrene due to the increased cross-linked density of the resulting IPN (Table 2). Thus, IPN IS1A showed the maximum hardness, as it has the maximum CLF. A further increase in the PS content led to a decrease in the hardness, since the cross-link density of the IPNs decreased with increasing PS content.

The tensile properties of the IPNs are dependent on the cross-link density and the efficiency of stress transfer between the PU and the PS networks. Since polymers are viscoelastic materials, the tensile properties are dependent on the rate of deformation. The tensile properties of the IPNs such as initial modulus, elongation at break, and tensile strength at break were determined at two deformation rates. The results are summarized in Table 2.

The stress–strain curves of all the IPNs at the higher deformation rate of 125% elongation/min are shown in

Table 2. Hardness and Tensile Properties of IPNs

code	hardness (Shore A)	initial modulus (kg/cm²)		tensile strength (kg/cm²)		elongation at break (%)		recovery[a] (%)
		A[a]	B[b]	A[a]	B[b]	A[a]	B[b]	
PU-2	27	180	29	45	21	38.7	83	100
IS1A	84	1827	113	156	71	22.0	75	94
IS1B	74	988	61	146	58	29.0	78	92
IS1C	70	717	46	143	65	29.5	122	89
IS1D	66	436	29	104	49	39.0	158	81

[a] Tensile measurements at a deformation rate of 125% elongation/min. [b] Tensile measurements at a deformation rate of 50% elongation/min.

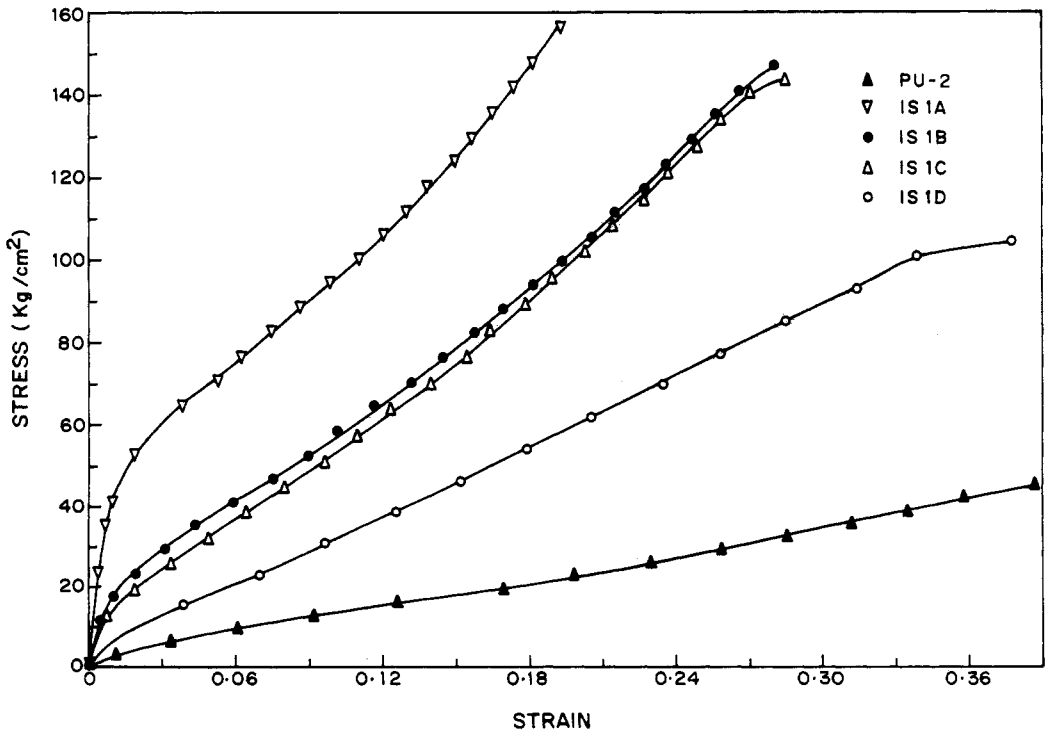

Figure 2. Stress–strain behavior of interconnected IPNs at a deformation rate of 125% elongation/min.

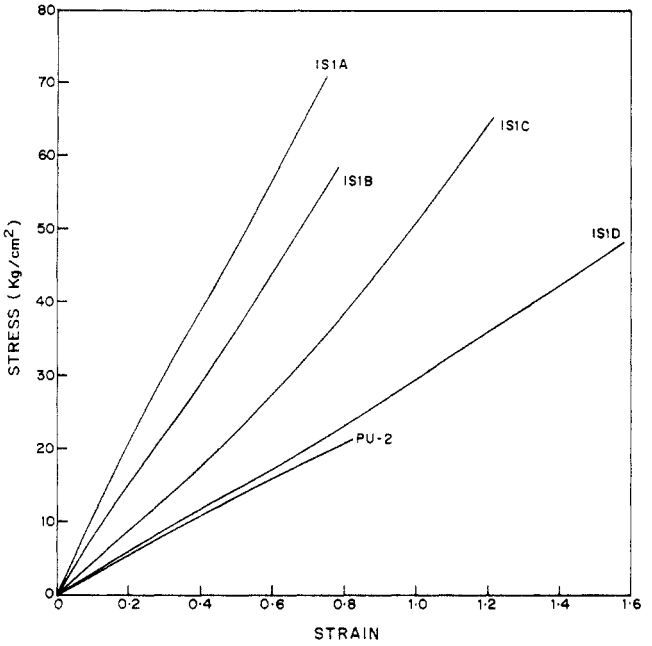

Figure 3. Stress–strain behavior of interconnected IPNs at a deformation rate of 50% elongation/min.

Figure 2. The PU network PU-2 shows a typical elastomeric behavior. There is a significant increase in the tensile strength at break and the modulus with only 10% addition of styrene to the PU network, while the elongation at break decreased. On a further increase in the styrene content up to 30%, both the tensile strength at break and modulus decreased and the elongation at break increased. For the 50/50 PU/PS IPN, IS1D, there was a further significant drop in modulus and strength. IS1D showed stress whitening near the site of breaking. This indicates that void formation has taken place during deformation of the IPN IS1D. Such a phenomenon was not observed in the case of the other IPNs. Stress whitening has also been observed for castor oil–polyurethane (COPU)/PS based IPNs at higher PS contents.[10] The base PU network, PU-2, showed elastomeric behavior, while the IPNs containing up to 30% PS behaved like a plastic and IPN IS1D behaved like a reinforced elastomer.

The base PU network is made up of a cage structure containing amorphous coiled chains. On deformation of PU, stresses are effectively distributed throughout the polymer network. Thus, PU shows elastomeric behavior. A sudden increase in the modulus and tensile strength at break on incorporation of 10% styrene can be explained on the basis of the stretched PS chains acting as intranetwork bridges, in the case of IS1A. Most of the applied stress was borne by these bridges, resulting in an increase in the modulus and tensile strength at break. At higher PS contents, the cross-link density of the IPNs decreases, resulting in a decrease in the tensile strength and the modulus.

The IPNs show similar changes in the tensile properties when tested at a lower deformation rate (Figure 3). However, the tensile strength at break and the modulus did not increase as significantly with the incorporation of a 10% PS network as observed at the higher deformation rate. This was due to the lower deformation rate of this experiment which allows more efficient stress relaxation. It may be noted that the modulus of the PU network PU-2 and that of IPN IS1D are of the same order at lower deformation rate. This implies that in IS1D the PS bridges are able to transfer the stress effectively to the PU network due to the formation of a collapsed cage structure.

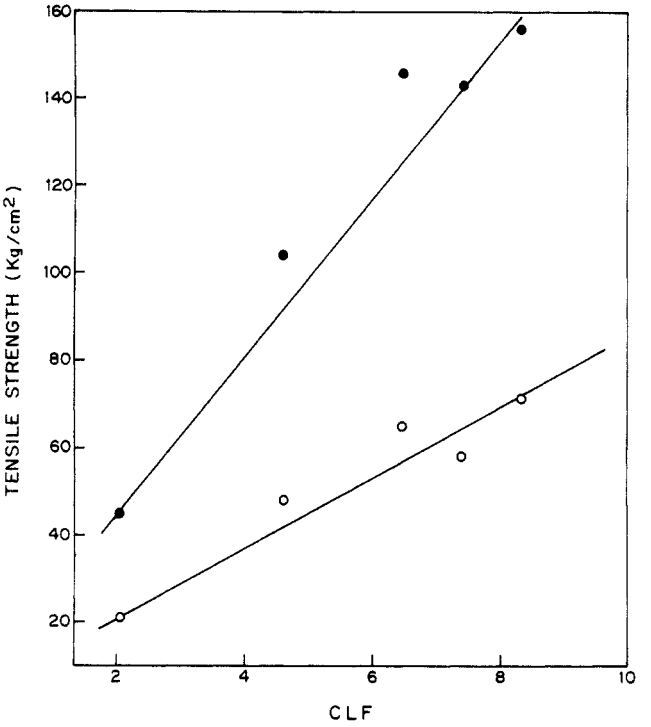

Figure 4. Effect of the cross-link factor (CLF) on the tensile strength at deformation rates of 125% and 50% elongation/min.

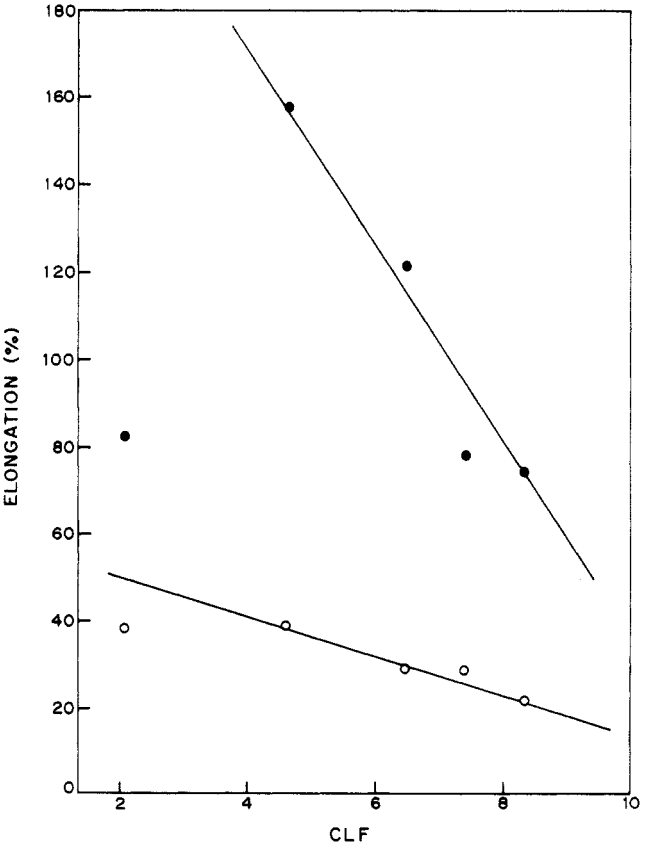

Figure 5. Effect of the cross-link factor (CLF) on the elongation at break of interconnected IPNs at deformation rates of 125% and 50% elongation/min.

As shown in Figures 4 and 5, the tensile strength and elongation at break of the IPNs at a deformation rate of 125% elongation/min were found to vary linearly with the cross-link factor, CLF, indicating that the mechanical behavior of these IPNs is highly dependent on the cross-link density of the network. While, at a lower deformation rate of 50% elongation/min, although a good correlation

Table 3. Dynamic Mechanical Properties of IPNs

code	temp at $G' = 1 \times 10^{10}$ (°C)	glass transition temp T_g (°C)	tan δ_{max}	$10^{-9}G''_{max}$ (dynes/cm^2)	G''_{max} temp (°C)	M_c
PU-2	7	41	1.1250	1.40	19	11976
IS1A	0	38	0.8392	1.51	9	4940
IS1B	−5	39	0.8542	1.41	10	6800
IS1C	3	48	0.9728	1.12	21	7779
IS1D	1	36, 110[a]	0.7713, 0.2518[a]	1.48	10	3186

[a] Values corresponding to T_g of the PS phase.

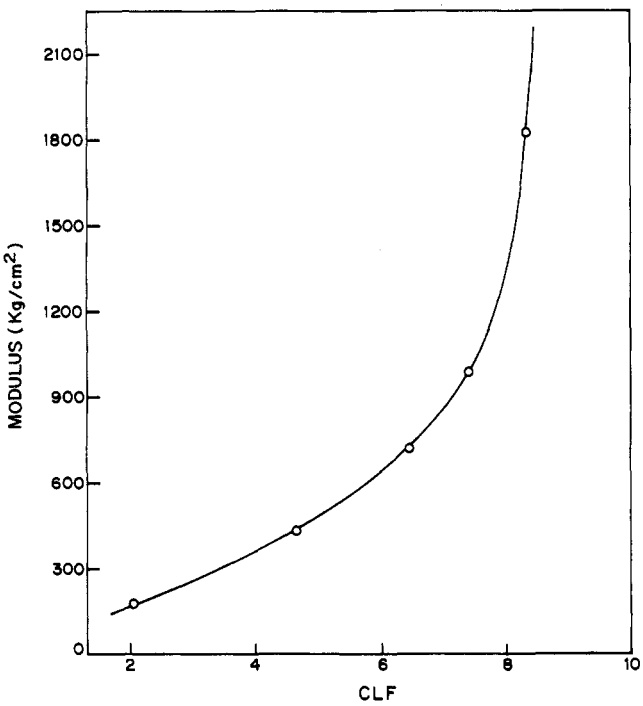

Figure 6. Effect of the cross-link factor (CLF) on the modulus of interconnected IPNs at a deformation rate of 125% elongation/min.

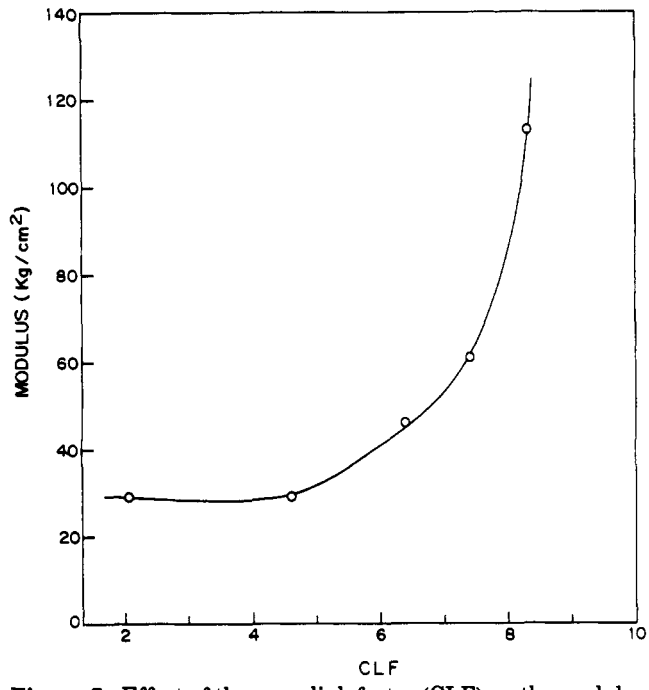

Figure 7. Effect of the cross-link factor (CLF) on the modulus of interconnected IPNs at a deformation rate of 50% elongation/min.

between CLF and the tensile strength and elongation at break was observed (Figures 4 and 5), the elongation at break of the base PU network, PU-2, was much lower than that expected by the linear behavior.

The modulus of the IPNs increased exponentially with increasing CLF (Figures 6 and 7). This shows that, with an increase in the CLF, the tensile behavior of the IPNs changes from a stress limiting mechanism to a strain limiting mechanism. Thus, the external stresses are taken up by the hard PS network chain segments. These do not transfer the stresses effectively to the PU network. As a result, the stress relaxation from the PS network to PU network is decreased with an increase in the cross-link density of the IPN. The highest moduli are obtained in the cases of IPNs IS1A and IS1B where the PS bridges are short and highly stretched.

The difference between the tensile properties of the IPNs at two deformation rates arises due to the rate of stress transfer from PS bridges to the PU network. The large change in the modulus was observed at a higher deformation rate while at a lower deformation rate the moduli did not change appreciably. This implies that the relaxation time of the IPNs was such that only at a lower deformation rate are the stresses efficiently distributed between the two networks.

Higher tensile strengths of IS1C at both the deformations rates than that of IS1B, in spite of a lower cross-link density (lower CLF), are attributed to the increased rigidity of this IPN due to the presence of crystalline domains of polyether chain segments.[8] This effect of the presence of crystalline domains was not observed in the case of the initial modulus, indicating that the network stresses are mainly distributed on intranetwork PS bridges and the stress relaxation process was not significantly altered due to the presence of these crystalline domains.

In the case of IS1D, the percent recovery was very low (see Table 2). This is the effect of the collapsed cage morphology of IS1D. During tensile deformation, the coiled chains of PS are stretched and they do not revert back to the coiled chain configuration after removal of the stress. This result is consistent with the WAXD data, reported in an earlier communication,[8] which showed that the d_{eff} increased to 4.15 Å after the stretching versus 3.96 Å before the irreversible tensile deformation.

Dynamic Mechanical Analysis. The results of the dynamic mechanical analysis are summarized in Table 3. The IPNs, PU-2 through IS1C, showed only PU glass transition temperatures (T_g's), as indicated by the tan δ peak temperature (Figure 8). However, IPN IS1D showed two separate T_g's for the PU and PS phases. A single T_g for PU-2 is expected due to the presence of only the PU phase. In the case of IPNs IS1A, IS1B, and IS1C, the PS intranetwork bridges are in a stretched configuration. Therefore the PS chains present in these IPNs would be more rigid as compared to those of the homopolymer PS.[9] Thus, the T_g of the PS phase is expected to be much higher than the T_g of the homopolymer PS containing PS chains in a coiled configuration. Therefore, in the selected temperature range −70 to +130 °C, the T_g of the PS phase might not have been observed. In the case of IPN IS1D, the PS bridges are in a coiled configuration and would

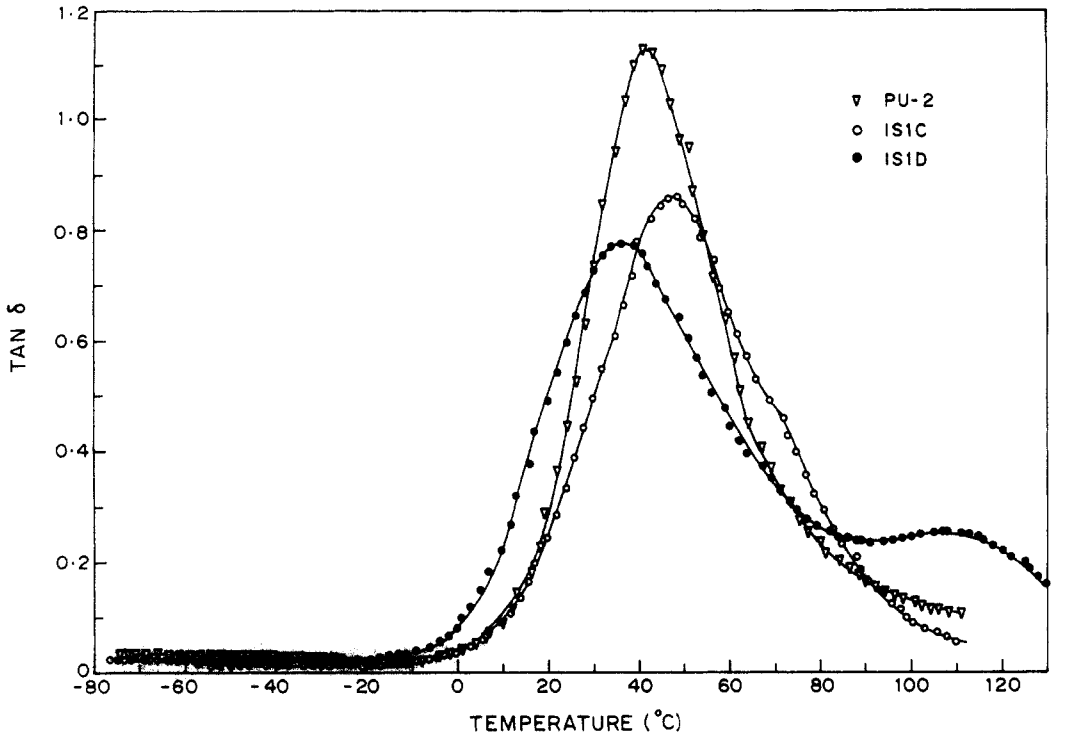

Figure 8. tan δ variation of interconnected IPNs.

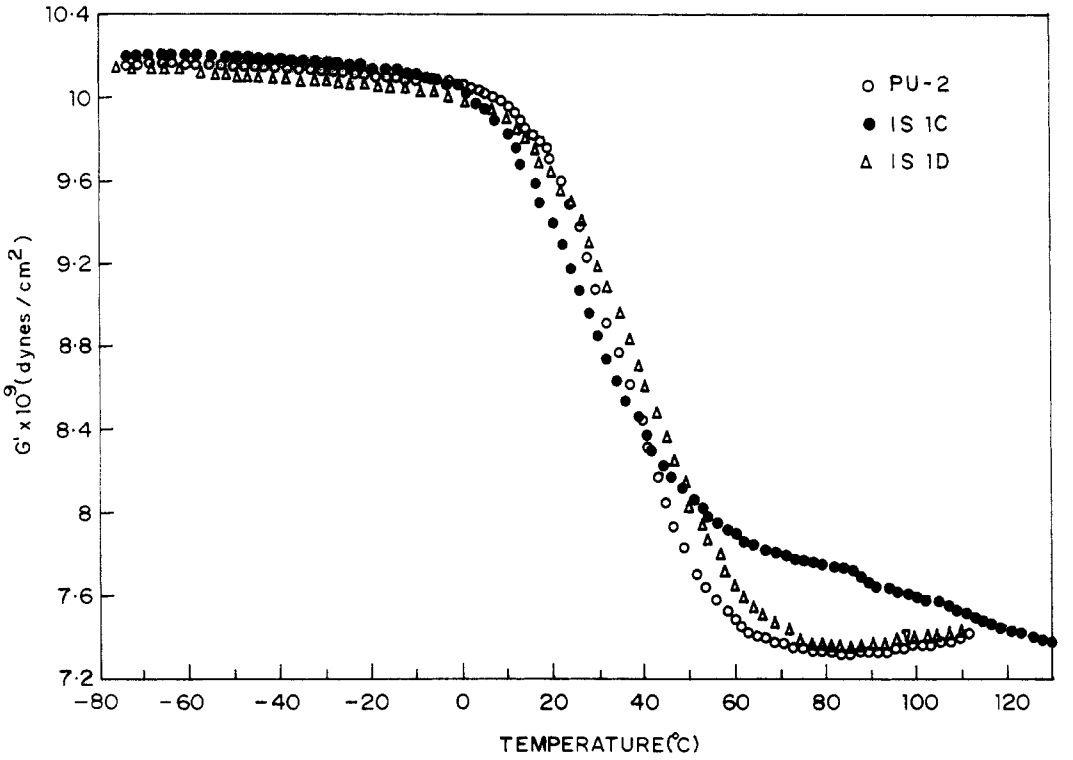

Figure 9. G' variation of interconnected IPNs.

manifest greater mobility, thereby lowering the T_g. Thus, the T_g's of both the PU and PS phases were observed in the case of IPN IS1D at 36 and 110 °C, respectively (Figure 8). The T_g of the base PU, PU-2, was 41 °C, while IPNs IS1A, IS1B, and IS1D exhibited T_g's around 36–39 °C. This marginal lowering the T_g can be attributed to the increased free volume of these IPNs. The higher T_g of the PU phase of IS1C (T_g = 48 °C) relative to that of other IPNs is due to the formation of crystalline domains of the polyether chain segments of the PU chains, thereby hindering the main chain motion.[11]

The tan δ curve shows a decrease of about 25% in the value of tan δ_{max} on addition of 10% PS to the PU network. This is due to the increased cross-link density of the IPN. However, a further increase in the PS content decreased the cross-link density of the polymer, leading to a gradual increase in the tan δ_{max} value. In the case of IS1D, a different behavior is observed, as a result of a change in the morphology of the sample.

The variation of the storage modulus (G') with temperature is shown in Figure 9. The temperature at which the value of G' reached 1×10^{10} is reported in Table 3. The G' of the PU network PU-2 reached 1×10^{10} at a temperature of 7 °C. However, in the case of IPNs IS1A through IS1D containing PU as well as PS phases, the value of G' reached 1×10^{10} at temperatures around −5

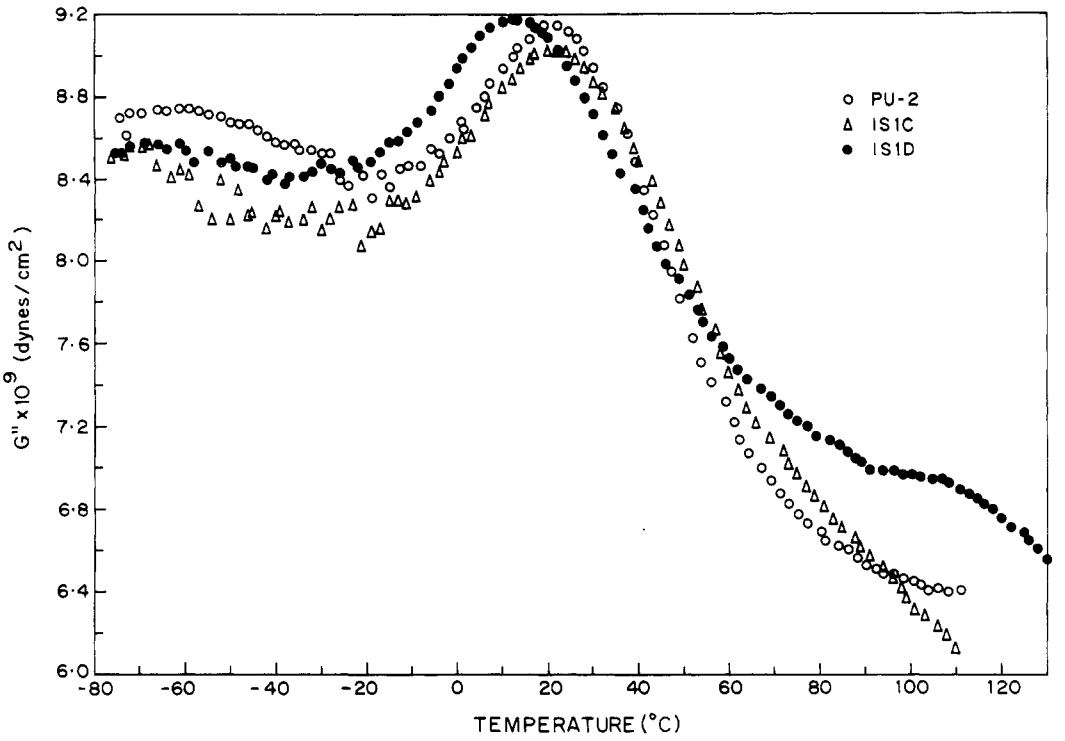

Figure 10. G'' variation of interconnected IPNs.

to +3 °C. This slight drop in the temperature is attributed to the increase free volume of these IPNs. The negligible change in the temperatures in spite of the presence of the rigid PS phase shows that the presence of PS does not hinder the mobility of the PU chains. Thus these IPNs have formed a structure similar to that of the block copolymer, implying that the PS phase is present as bridges, formed between the PU network chains.

The variation of loss modulus (G'') with temperature is shown in Figure 10. The G'' curve for IPN PU-2 shows two peaks at −65 and +19 °C. The α-transition peak at 19 °C is observed due to the main chain motion of the PU network, and the β-transition peak at −65 °C is observed due to segmental motion of the polyether chain segments. In the case of IPNs IS1A and IS1B α- and β-transitions were observed at −65 and +9–10 °C, respectively. Lowering of the α-transition temperature is attributed to the increased free volume of these IPNs. In the case of IPN IS1C the α-transition peak was observed at 21 °C due to the presence of crystalline domains. Also, due to crystallization of polyether chain segments, the β-transition was observed at −69 °C. Also, a much lower value of G''_{max} was observed for the β-transition. IPN IS1D showed three peaks at −65, +10, and +110 °C, corresponding to the β-transition of the PU network, the α-transition of the PU network, and the α-transition of the PS phase, respectively.

The molecular weight between cross-links (M_c) of the IPNs was measured using the following equation:[12]

$$G' = dRT/M_c \qquad (2)$$

where d is the density of the IPN, R is the gas constant, T is the absolute temperature at 40 °C higher than the T_g of the IPN, and G' is the value of the storage modulus at T. The values of M_c obtained by using this equation are listed in Table 3. It can be seen that there is a sharp decrease in M_c with 10% styrene addition due to the intranetwork bridge formation, whereas beyond 10% styrene, the value of M_c increased with increasing styrene content since the bridge length was also increased. Thus, the changes in the M_c show a trend similar to the CLF of IPNs. Also, a similar effect on the value of M_c was observed by Kumar et al.[13] in the case of COPU/PS IPNs.

Table 4. Permeabilities and Permselectivities of IPNs

code	pressure (psi)	$10^{-12}P_{N_2}$ (cm³ (STP)·cm/cm²·s·cmHg)	$10^{-10}P_{CO_2}$ (cm³ (STP)·cm/cm²·s·cmHg)	P_{CO_2}/P_{N_2}
PU-2	300	5.2	4.8	92
	350		5.8	
	400		6.6	
IS1A	300	4.4	3.6	83
IS1C	200		5.4	
	312	4.9	4.4	89
	400		2.5	
IS1D	300	3.0	2.5	84

Permeability. The permeation of gases is a result of the sorption and diffusion of the gases through the polymer. The permeability P is given by

$$P = DS \qquad (3)$$

where D denotes the diffusivity and S is the solubility of the gas in the polymer. Diffusion of the gases through the IPNs would mainly be dependent on the IPN cage structure, free volume, and the size of the penetrant moiety, while the solubility would be dependent on the polymer–gas interaction and the free volume. The permeability of N_2 and CO_2 gases through IPNs was studied at various pressures. N_2 is a comparatively inert gas and would interact weakly with the IPNs. Thus, the variation in permeability through various IPNs would be mainly governed by the changes in diffusivity. CO_2 is a polar gas which would interact strongly with the IPN. Thus, its permeability would be influenced by both diffusivity as well as solubility.

The permeabilities of N_2 and CO_2 through the IPNs at various pressures are tabulated in Table 4. It was observed that the permeability of N_2 through the IPNs was much lower than the permeability of CO_2. The ratios of pure gas permeabilities were in the range 84–90 for all the IPNs. These values are higher than the selectivities of some known highly selective glassy polymers like polyimides.[14]

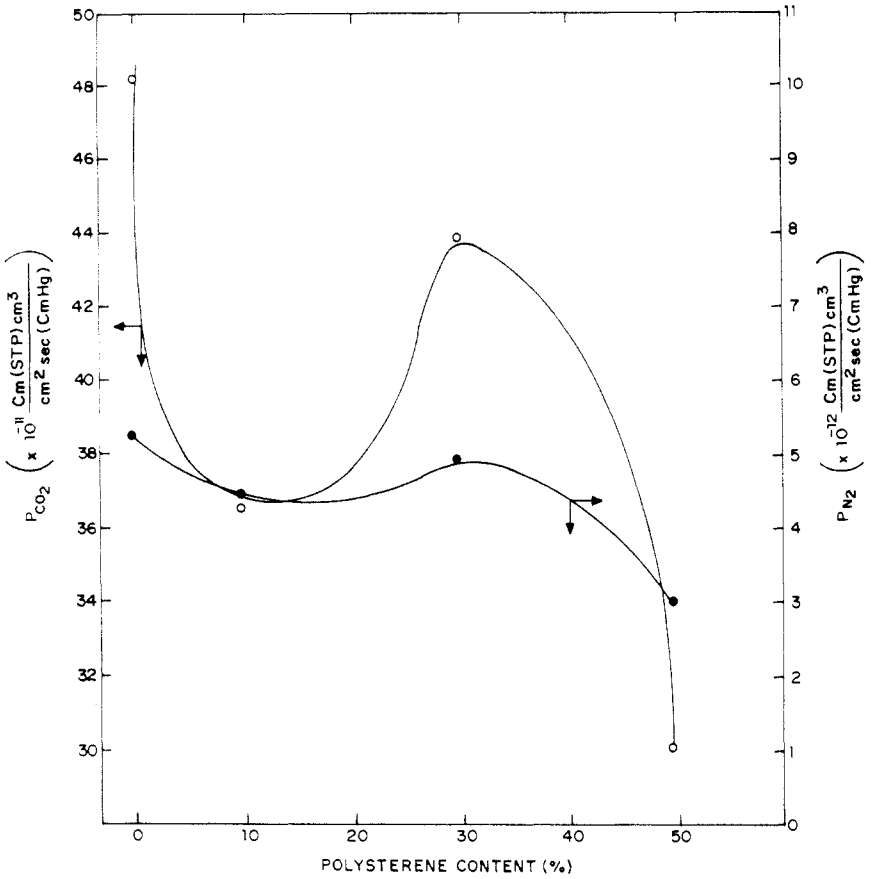

Figure 11. Variation in permeabilities of N_2 and CO_2 with the PS content in interconnected IPNs.

The permeability of CO_2 through PU-2 and IS1C was measured at various pressures. In the case of the base PU, PU-2, the permeability increased with pressure. Thus, plasticization of the base PU network by the CO_2 gas increases the flux of gas passing through the network. Such a behavior is typical of an elastomeric material. In the case of one IPN, IS1C, the CO_2 permeability decreased with increasing pressure. This shows that plasticization of the network of the IPN IS1C did not take place due to the presence of the stretched PS bridges. Thus, IS1C exhibits a behavior typical of glassy polymers.

On incorporation of 10% PS in the base PU, the effective distance between the chains d_{eff} (see Table 1) of the IPN IS1A increased from 4.04 to 4.15 Å. However, the permeabilities of both the gases, N_2 and CO_2, through IS1A were lower than those in the base PU, PU-2 (Figure 11). The lowering of the permeability in IS1A is attributed to an increase in the IPN cross-link density (as indicated by the CLF) through intranetwork bridge formation. This was observed in spite of the permeability of N_2 in PS being 10 times higher than that observed for the PU network PU-2.[15] This shows that the PS is incorporated in the PU matrix as intranetwork bridges and is not present as a separate phase. A further increase in the PS content up to 30% led to an increase in the cage size due to the longer PS bridge formation. This larger cage size led to an increase in the permeability of both the gases through IS1C. IPN IS1D showed a large drop in the flux of both the gases due to the formation of a collapsed cage morphology with a decreased d_{eff}. This adversely affected the transport of both gases through the membrane.

It was observed that the changes in permeability of N_2 and CO_2 through the IPNs with respect to the base PU, PU-2, can be empirically correlated with d_{eff} and CLF using the following linear equation:

Table 5. Degradation Behavior of IPNs[a]

code	T_i (°C)	$T_{1_{max}}$ (°C)	$T_{2_{max}}$ (°C)	$T_{3_{max}}$ (°C)	T_f (°C)
PU-2	261	386		626	710
IS1A	227	359		606	696
IS1B	250	365		599	701
IS1C	237	370		587	701
IS1D	253	354	394	557	657

[a] T_i, initial degradation temperature; $T_{1_{max}}$, temperature at maximum degradation rate for peak 1; $T_{2_{max}}$, temperature at maximum degradation rate for peak 2; $T_{3_{max}}$, temperature at maximum degradation rate for peak 3; T_f, final degradation temperature.

$$\ln\left[\frac{P}{P_{IS1A}}\right] = m \ln\left[\frac{d_{eff}}{d_{eff_{IS1A}}}\right] - n \ln\left[\frac{CLF}{CLF_{IS1A}}\right] \quad (4)$$

where P is the permeability, d_{eff} is the effective distance between the adjacent chains, and CLF is the cross-link factor. A good correlation between observed and predicted permeability was obtained. The permeability of the gases through these IPNs is decreased by increasing the cross-link density. Also the morphology of the IPNs affects d_{eff} and therefore the flux.

In order to study the constraints forced by the PS bridges on the diffusion of gas, nitrogen was selected because it is a nonpolar gas. The permeability of nitrogen through IS1C was measured at various temperatures (Figure 12). The activation energy of the nitrogen passage through IS1C was 13.4 kcal/mol, a value which is higher than the reported values of 10–11 kcal/mol.[15] The higher value of the activation energy for the passage of N_2 was observed due to the cage formed by two highly flexible chains of PU and two rigid chains of PS.

Thermogravimetric Analysis. The results of thermogravimetric analysis are summarized in Table 5. The percentage weight loss as a function of temperature is shown in Figure 13. The initial degradation temperature

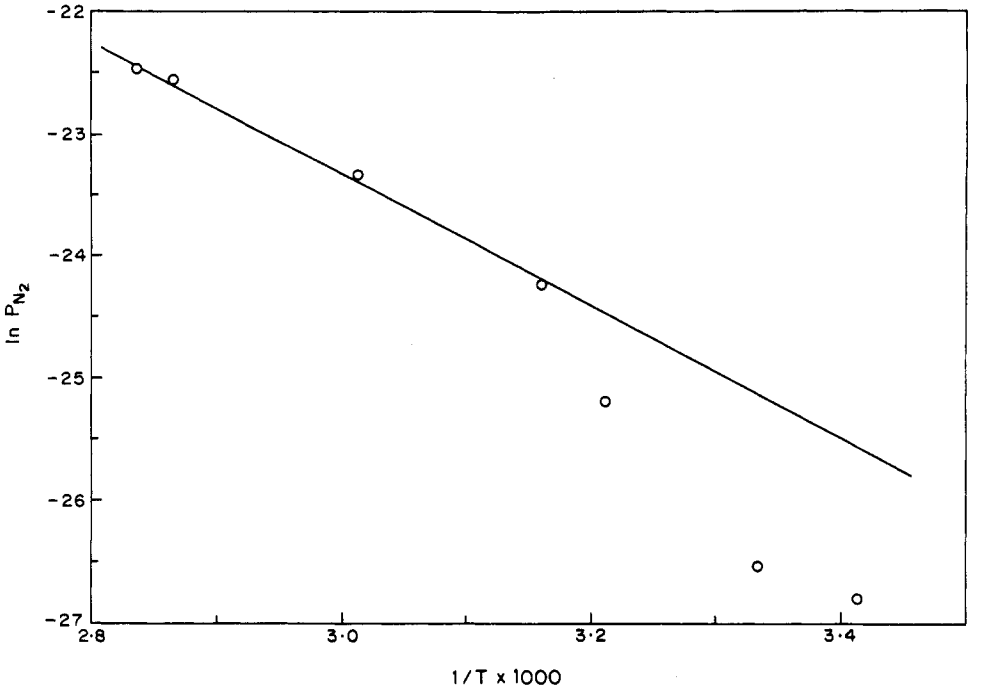

Figure 12. Activation energy of N_2 passage through IS1C.

(T_i) of the base PU network, PU-2, was 261 °C. However, on addition of 10% styrene the initial degradation temperature decreased to 227 °C. This is attributed to an increase in the cross-link density by formation of PS intranetwork bridges which led to formation of strained bonds. On further addition of styrene to 20% and 30%, the initial degradation temperature increased to 250 and 237 °C, respectively. Although the bonds present in these IPNs are expected to be more strained, the increase in the initial degradation temperature on further addition of the PS led to formation of a crystalline phase which led to increased thermal stability. The increased initial degradation temperature at 50% styrene content is due to the formation of a collapsed cage structure.

The differential thermograms (DTG—dw/dT vs temperature) of the IPNs are shown in Figure 14. The base PU network, PU-2, showed two degradation peaks at 386 and 626 °C, respectively. In the case of IPN IS1D three degradation peaks were observed at 354, 394, and 557 °C. The appearance of the third peak at 394 °C is assigned to the degradation of the PS phase. In the case of IPNs IS1A, IS1B, and IS1C, the degradation peaks of PU and PS are present; however they are not well separated and the gradual appearance of a second peak around 360–390 °C was evident as the PS content is increased.

The degradation temperature of the first peak ($T_{1_{max}}$) shows a trend similar to that in the case of T_i. The highest $T_{1_{max}}$ (386 °C) was observed for the base PU network. On addition of 10% styrene the lowest degradation temperature (359 °C) was observed due to increased cross-link density and the presence of strained bonds. However, due to lowering of the cross-link density of the IPN on further addition of PS, higher degradation temperatures were observed in case of IS1B and IS1C. The sudden decrease in the degradation temperature when the PS content was increased from 30 to 50% was observed since the IPNs containing up to 30% styrene content overlapped peaks of the PS degradation which increased the apparent maximum degradation temperature. The degradation temperature of the third peak $T_{3_{max}}$ decreased continuously with an increase in the PS content. Thus, the degradation

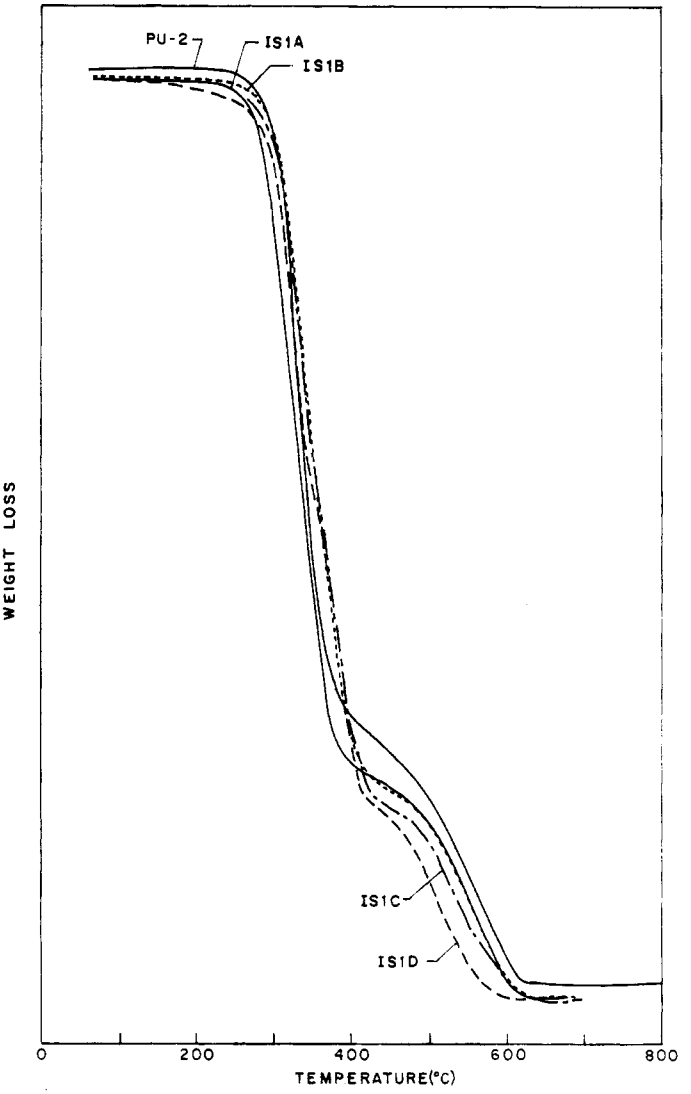

Figure 13. Thermal degradation behavior of interconnected IPNs.

behavior of the IPNs IS1A, IS1B, and IS1C showed the presence of weakened bonds. This is attributed to the

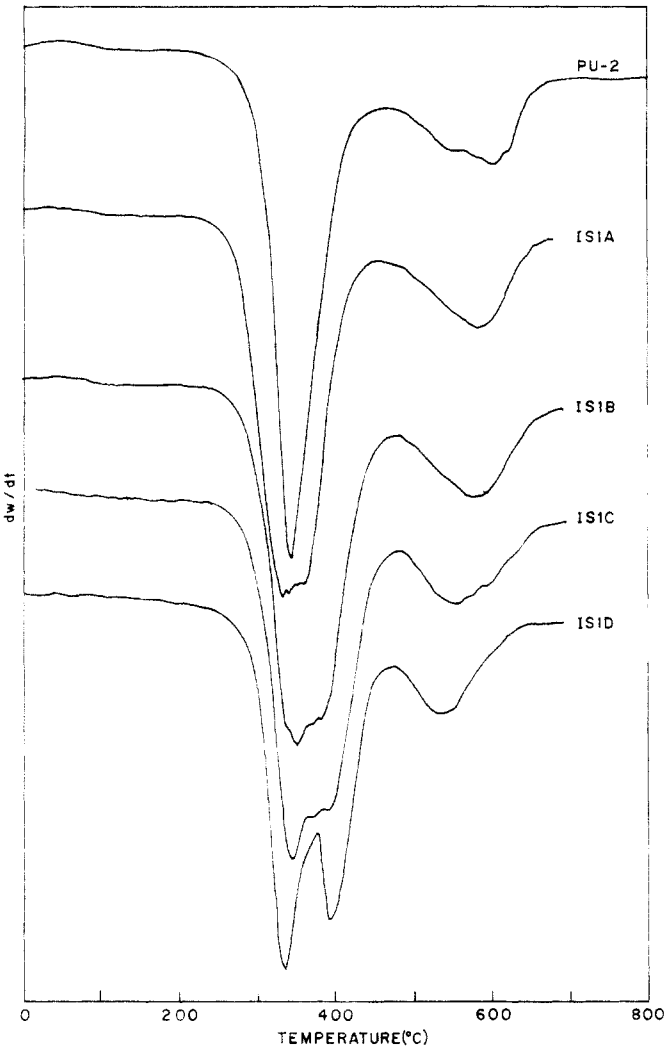

Figure 14. DTG of interconnected IPNs.

strain points developed due to cage stretching, which can break easily by the supply of thermal energy.

Conclusions

It was observed that the tensile properties of the IPNs at higher and lower deformation rates can be rationalized on the basis of the proposed hypothesis. Also, it was shown that the modulus of these IPNs is highly sensitive to the rate of stress transfer from rigid polymer to soft polymer. As a result of coiled configuration of the PS, bridges in IPN IS1D exhibited less tensile recovery. The dynamic mechanical properties of the IPNs IS1A, IS1B, and IS1C showed a single T_g corresponding to the PU phase due to the presence of stretched PS intranetwork bridges. The T_g's of both PU and PS phases were observed in the case of IS1D due to the coiled configuration of the PS bridges. The T_g of the PU phase in the case of IPN IS1C was high due to the formation of crystalline domains. The dependence of the molecular weight between cross-links (M_c) of the IPNs on the PS concentration showed a trend similar to that of the CLF. The permeability of various gases through these IPNs is rationalized on the basis of morphology and the cross-link density of these IPNs. A higher activation energy was observed for the passage of N_2 through the IPN because of the presence of stretched PS bridges. The inferior thermal properties exhibited by these IPNs are explained on the basis of formation of the strained bonds.

References and Notes

(1) (a) Sperling, L. H. *Interpenetrating Polymer Networks and Related Materials*: Plenum: New York, 1981. (b) Sperling, L. H. *Contemp. Top. Polym. Sci.* **1986**, *6*, 665. (c) Sperling, L. H.; Fay, J. J.; Murphy, C. J.; Thomas, D. A. *Makromol. Chem., Macromol. Symp.* **1990**, *38*, 99.

(2) (a) Frisch, H. L.; Klempner, D.; Frisch, K. C. *J. Polym. Sci.* **1969**, *B7*, 775. (b) Klempner, D.; Kwei, T. K.; Matsuo, M.; Frisch, H. L. *J. Polym. Sci., Polym. Phys. Ed.* **1970**, *8*, 921. (c) Sperling, L. H.; Taylor, D. W.; Kirckpatrick, M. L.; George, H. F.; Berdman, D. R. *J. Appl. Polym. Sci.* **1970**, *14*, 73.

(3) (a) Sperling, L. H.; Friedman, D. W. *J. Polym. Sci., Polym. Phys. Ed.* **1969**, *7*, 425. (b) Shibayama, K.; Suzuki, Y. *Kobunshi Kogatu* **1966**, *23*, 24. (c) Fay, J. J.; Thomas, D. A.; Murphy, C. J.; Sperling, L. H. *Polym. Mater. Eng. Sci.* **1990**, *63*, 493. (d) Idem. *Makromol. Chem., Macromol. Symp.* **1990**, *38*, 99. (e) Fox, R. B.; Bitner, J. L.; Hinkley, J. A.; Carter, W. *Polym. Eng. Sci.* **1985**, *25* (3), 157. (f) Frisch, H. L.; Frisch, K. C. *Prog. Org. Coat.* **1979**, *7*, 105.

(4) (a) Balyakov, V. K.; Berlin, A. A.; Bukin, I. I.; Orlov, V. A.; Tarakanol, O. G. *Polym. Sci. USSR* **1968**, *10*, 700. (b) Frisch, K. C.; Klempner, D.; Antczak, T.; Frisch, H. L. *J. Appl. Polym. Sci.* **1974**, *18*, 683.

(5) (a) Lee, D. S.; Kang, W. K.; An, J. H.; Kim, S. C. *J. Membr. Sci.* **1992**, *75*, 231. (b) Chen, S. A.; Ju, H. L. *J. Appl. Poly. Sci.* **1980**, *25*, 1105. (c) Frisch, H. L.; Cifaratti, J.; Palma, R.; Schwartz, R.; Foreman, R.; Yoon, H.; Klempner, D.; Frisch, K. C. In *Polymer Alloys*: Frisch, K. C., Eds.; Klempner, D., Plenum Press: New York, 1977.

(6) Scarito, P. R.; Sperling, L. H. *Polym. Eng. Sci.* **1979**, *19*, 297.

(7) Frisch, H. L.; Frisch, K. C.; Klempner, D. *Polym. Eng. Sci.* **1974**, *14*, 646.

(8) (a) Pandit, S. B. Ph.D. Thesis, University of Poona, 1992. (b) Pandit, S. B.; Nadkarni, V. M. *Ind. Eng. Chem. Res.* **1993**, *32* (12), 3089. (c) Pandit, S. B.; Nadkarni, V. M. *Macromolecules*, in press.

(9) (a) Houde, A. Y. Ph.D. Thesis, University of Poona, 1991. (b) Stern, S. A.; Gareis, P. J.; Sinclair, T. F., Mohr, P. H. *J. Appl. Polym. Sci.* **1963**, *7*, 2035.

(10) Lipatov, Yu. S.; Shilov, V. V.; Bogdanovich, V. A.; Karabanova, L. V.; Sergeeva, L. M. *Kompoz. Polim. Mater.* **1981**, *10*, 3.

(11) Murayama, T. *Dynamic Mechanical Analysis of Polymeric Materials*: Materials Science Monographs 1; Elsevier Scientific Publishing Co.: New York, 1978.

(12) Murayama, T.; Bell, J. P. *J. Polym. Sci., Polym. Phys. Ed.* **1970**, *8*, 437.

(13) Kumar, V. G.; Rao, M. Rama; Guruprasad, T. R.; Rao, K. V. C. *J. Appl. Polym. Sci.* **1987**, *34*, 1803.

(14) Cabasso, Israel. *Encyclopedia of Polymer Science and Engineering*, 2nd ed.; John Wiley and Sons: New York, 1987; Vol. 9, p 509.

(15) Stannett, V. In *Diffusion in Polymers*: Crank, J., Park, G. S., Eds.; Academic Press: Amsterdam, Holland, 1975.